Comparative urine metabolomics of mice treated with non-toxic and toxic oral doses of (-)-epigallocatechin-3-gallate

Journal:	*Food & Function*
Manuscript ID	FO-ART-07-2023-002710.R1
Article Type:	Paper
Date Submitted by the Author:	26-Sep-2023
Complete List of Authors:	Hwang, Soomee; Penn State University, Food Science Koo, Imhoo; The Pennsylvania State University, Molecular Toxicology Patterson, Andrew; The Pennsylvania State University, Molecular Toxicology Lambert, J.; Penn State University, Food Science

Comparative urine metabolomics of mice treated with non-toxic and toxic oral doses of (-)-epigallocatechin-3-gallate

Soomee Hwang[a], Imhoi Koo[b], Andrew D. Patterson[b,c], Joshua D. Lambert[a,c,*]

[a] *Department of Food Science, The Pennsylvania State University, University Park, PA 16802, USA*

[b] *Department of Veterinary and Biomedical Sciences, The Pennsylvania State University, University Park, PA 16802, USA*

[c] *Center for Molecular Toxicology and Carcinogenesis, The Pennsylvania State University, University Park, PA 16802, USA*

*Corresponding author. Department of Food Science, Center for Molecular Toxicology and Carcinogenesis, The Pennsylvania State University, 332 Food Science Building, University Park, PA 16802, USA. Tel.: +1 814 865 5223. Email address: jdl134@psu.edu

Abstract

The green tea polyphenol, (-)-epigallocatechin-3-gallate (EGCG), has been studied for its potential positive health effects, but human and animal model studies have reported potential toxicity at high oral bolus doses. This study used liquid chromatography-mass spectrometry-based metabolomics to compare the urinary EGCG metabolite profile after administration of a single non-toxic (100 mg/kg) or toxic (750 mg/kg) oral bolus dose to male C57BL6/J mice to better understand how EGCG metabolism varies with dose. EGCG metabolites, including methyl, glucuronide, sulfate, and glucoside conjugates, were tentatively identified based on their mass to charge (*m/z*) ratio and fragment ion patterns. Partial least squares discriminant analysis (PLS-DA) results showed clear separation of the urine metabolite profiles between treatment groups. The most differentiating metabolites in the negative and positive ion modes were provisionally identified as di-glucuronidated EGCG quinone and di-glucuronidated EGCG, respectively. The presence of EGCG oxidation products at toxic dose is consistent with studies showing that EGCG toxicity is associated with oxidative stress. Relative amounts of methylated metabolites increased with dose to a lesser extent than glucuronide and sulfate metabolites,

indicating that methylation is more prominent at low doses, whereas glucuronidation and sulfation may be more important at higher doses. One limitation of the current work is that the lack of commercially-available EGCG metabolite standards prevented absolute metabolite quantification and identification. Despite this limitation, these findings provide a basis for better understanding the dose-dependent changes in EGCG metabolism and advance studies on how these differences may contribute to the toxicity of high doses of EGCG.

Keywords: green tea; (-)-epigallocatechin-3-gallate; mice; metabolomics; biotransformation

24 **1. Introduction**

25 Green tea (*Camellia sinensis*, Theaceae) is a widely consumed beverage with a long
26 history of safe consumption. Epigallocatechin-3-gallate (EGCG), the most abundant catechin in
27 green tea, has been reported to have potential cancer preventive, anti-inflammatory, and obesity
28 preventive effects [1, 2]. However, safety concerns about the oral bolus intake of EGCG have been
29 reported in laboratory animal studies. Isbrucker et al. investigated the toxicity of repeated dose of
30 EGCG in fasted dogs and observed that a bolus dose of 500 mg EGCG /kg/d caused vomiting
31 and diarrhea in all dogs, as well as morbidity in a few dogs during the study [3]. Green tea extract
32 (GTE) and EGCG have both been shown to cause treatment-related mortality in mice after the
33 oral bolus administration [4-7]. For example, a study from our laboratory has shown that once-daily
34 oral bolus dosing with EGCG (0 – 750 mg/kg/d) dose-dependently increased plasma alanine
35 aminotransferase (ALT) levels, markers of hepatic oxidative stress, and incidence/severity of
36 hepatic necrosis [7]. These effects were associated with mitochondrial swelling and decreased
37 mitochondria number. A recent meta-analysis of 159 human clinical trials evaluating the health
38 effects of green tea, GTE, and EGCG found 11 studies that reported elevated serum liver
39 enzymes. The authors found an overall incidence rate for adverse events of 7.0%. In all cases,

40 adverse effects were associated with the use of solid bolus dosage forms rather than green tea
41 beverages. In addition, more than 40 case reports of human hepatotoxicity associated with the
42 use of green tea-based supplements have been reported since 1999 [8].

43 The Minnesota Green Tea Trial represents the longest duration study to report adverse
44 hepatic events. Women who received GTE (containing 843 mg EGCG) for 1 year had increased
45 incidence of elevated plasma ALT levels compared to placebo treated subjects (6.7% vs. 0.07%)
46 [9]. Of these, 13 were classified as "moderate to severe" (3.1 – 20 times upper limit of normal
47 [ULN]) and 1 was classified as "life-threatening" (>20 times ULN). The authors also indicated
48 that cessation of treatment mitigated the elevations, whereas resumption of treatment in some
49 cases caused positive rechallenge [9]. While many studies on the potential health beneficial effects
50 of green tea and EGCG have been conducted, more research focused on dose-dependent EGCG
51 biotransformation is needed to determine if dose-dependent differences in biotransformation may
52 contribute to EGCG-mediated toxicity in humans and animals.

53 The major pathways of tea catechin biotransformation have been reported as methylation,
54 glucuronidation, and sulfation [10]. Meng et al., identified mono- and di-methylated EGCG in
55 human, mouse, and rat urine samples after tea or EGCG administration [11]. Mono-glucuronidated

56 EGCG has also been observed as one of the major metabolites both *in vivo* and *in vitro* [12, 13].

57 Sulfation of EGCG has not been well-studied, but EGCG-4″-sulfate has recently been identified

58 as a key metabolite in humans [14]. Products with multiple conjugations, such as glucuronide or

59 sulfate conjugates of methyl EGCG have also been observed in mouse urine samples following

60 EGCG administration [15].

61 A limited number of studies have shown that different metabolites are preferentially

62 produced at different EGCG dose levels. For example, Lu et al., suggested that glucuronidation

63 may be favored over methylation at the high dose of EGCG based on *in vitro* enzyme kinetics

64 studies [16]. Additionally, Sang et al., observed 2′-cysteinyl EGCG and 2″-cysteinyl EGCG in the

65 urine of mice only after the administration of high bolus doses of EGCG. These thiol conjugates

66 are hypothesized to be formed by a Michael Addition-type reaction between EGCG quinone and

67 glutathione, indicating that at high doses, EGCG quinones are formed *in vivo* [17].

68 Although the evolutionary goal of xenobiotic transformation is the inactivation and

69 elimination of potential toxicants from an organism, biotransformation can lead to the formation

70 of metabolites with greater toxic potential [18]. We have previously reported that 2″-cysteinyl-

71 EGCG has greater redox activity than EGCG *in vitro* suggesting that formation of this metabolite

72 is maladaptive [19]. Similar results have been previously reported for 3,4-

73 methylenedioxymethamphetamine which undergoes similar metabolism [20]. These observations

74 suggest that changes in EGCG metabolic profile at high doses may contribute to EGCG toxicity.

75 Given that EGCG is extensively metabolized, it is possible that at high doses, the normal

76 metabolic pathways are saturated, leading to the formation of unique metabolites or metabolite

77 profiles that have greater toxic potential. Most previous studies have focused on investigating the

78 metabolic fate of EGCG at non-toxic doses, and there is limited information on the metabolite

79 profile of EGCG at toxic doses. The aim of the present study was to compare the urine

80 metabolite profile using untargeted metabolomics in C57BL/6J mice following a single oral

81 gavage treatment with non-toxic or toxic doses of EGCG. EGCG metabolites were tentatively

82 identified based on their mass data, and multivariate statistical analysis was used to compare the

83 metabolite profiles of the treatment groups. To better understand how EGCG metabolism

84 changes with dose, we calculated the ratio of the averaged peak area of toxic to non-toxic groups

85 for the major conjugation types.

86

87 **2. Materials and methods**

88 *2.1. Chemicals and reagents*

89 EGCG (98% pure) was purchased from Cayman Chemical Co. (Ann Arbor, MI, USA). All

90 other reagents were of the highest grade commercially available.

91

92 *2.2. Animal treatment & Sample collection*

93 Animal studies were approved by the Institutional Animal Care and Use Committee of

94 the Pennsylvania State University (IACUC protocol no. 202001517). To compare the metabolite

95 profile of EGCG at different dose levels, 24 male C57BL6/J mice (5 weeks old, Jackson

96 Laboratory, Bar Harbor, ME, USA) were randomized into three treatment groups (n = 8 per

97 group) based on body weight: vehicle control group (0.9% sodium chloride); non-toxic dose

98 group (100 mg/kg EGCG); and toxic dose group (750 mg/kg EGCG). The toxic dose was

99 selected based on prior studies that have shown that daily treatment with 750 mg/kg EGCG by

100 oral gavage induced hepatotoxicity in mice [5, 7]. Mice were housed 4 per cage and given *ad*

101 *libitum* access to AIN93G diet and water prior to dosing. After 1 week of the acclimation period,

102 mice from the same home cage were pair housed in the metabolism cages (n = 2 per metabolism

103 cage) and further acclimated to the metabolism cages for 3 d. Mice were fasted for 7 h (0700 –

104 1400 h) prior to oral gavage administration of vehicle or EGCG. The urine was collected for 17 h

105 after treatment and frozen at -80˚C prior to preparation and analysis.

106

107 *2.3. Liquid chromatography-mass spectrometry method*

108 Prior to analysis, urine samples were combined with 2 volumes of methanol containing 1

109 μM chlorpropamide as an internal standard. After centrifugation, the supernatant was collected in

110 autosampler vials and stored at -20˚C before ultra-high performance liquid chromatography-

111 tandem mass spectrometry-based metabolomics analysis. Samples (5 µL) were separated using a

112 Prominence 20 UFLCXR system (Shimadzu, Columbia, MD, USA) equipped with a Waters

113 (Milford, MA, USA) BEH C18 column (2.1 × 100 mm, 1.7 µm particle size) maintained at 55˚C.

114 The mobile phase consisted of 0.1% aqueous formic acid (A) and acetonitrile containing 0.1%

115 formic acid (B). The initial solvent conditions were 3% B, increasing to 45% B at 10 min, 75% B

116 at 12 min, and held at 75% B until 17.5 min before returning to the initial conditions and re-

117 equilibrated for 2.5 min. The flow rate was 0.25 mL/min. The eluate was delivered into a

118 TripleTOF 5600 (QTOF) using a Duospray™ ion source (AB Sciex, Framingham, MA, USA).

119 The capillary voltage was set at 4 kV in negative ion mode and 5.5 kV in positive ion mode. The

120 mass spectrometer was operated with a full scan from 100 to 1250 mass-to-charge ratio (*m/z*)

121 (250 ms) followed by 10 tandem mass spectrometry (MS/MS) product ion scans (100 ms) per

122 duty cycle using a collision energy of 45 V with a 30 V spread.

123

124 *2.4. Comparison of urinary metabolite profiles between treatment groups*

125 Raw MS data including retention time (min) and *m/z* value were imported to MS-DIAL

126 (version 4.80, RIKEN CSRS, Yokohama City, Japan) for processing [21]. The processed dataset

127 was normalized and analyzed using MetaboAnalyst 5.0 (https://www.metaboanalyst.ca) [22]. To

128 compare the metabolite profiles between treatment groups, clustering analysis and partial least

129 squares-discriminant analysis (PLS-DA) were conducted. Variable Importance in Projection

130 (VIP) scores were used to determine the important features contributing to the discrimination in

131 the PLS-DA model. EGCG-related metabolites were tentatively identified based on their

132 molecular ion *m/z* and product ion patterns. Due to the lack of commercially-available standards

133 for EGCG metabolites, the ratio of the averaged peak area for each metabolite at the toxic and

134 non-toxic doses was calculated for relative quantification.

135 $$Ratio = \frac{[Metabolite\ Area]toxic}{[Metabolite\ Area]nontoxic}$$

136 The ratio was used to compare how the major conjugation types (methylation, glucuronidation,

137 and sulfation) varied with EGCG dose.

138

139 **3. Results and discussion**

140 *3.1 Tentative identification of the EGCG-related metabolites*

141 In this study, EGCG metabolites were tentatively identified based on the molecular ion

142 *m/z* and MS/MS spectra (Table 1). Most of the identified metabolites were methylated and/or

143 glucuronidated products. Although we cannot determine the exact structure of each compound

144 due to a lack of commercially-available authentic standards, the product ions of several

145 metabolites suggest possible conjugation sites. For example, MetNeg6 (rt = 3.6 min, *m/z* =

146 633.112) in negative ion mode that was tentatively identified as EGCG mono-glucuronide, the

147 presence of the characteristic ion at *m/z* 481 (mono-glucuronidated epigallocatechin) suggests

148 that the glucuronide is on the A- or B-ring rather than the galloyl moiety (Fig. S1). In the case of

149 MetNeg8 (rt = 4.4 min, *m/z* = 633.113), which is also tentatively identified as mono-

150 glucuronidated EGCG, the presence of the product ion at *m/z* 345 (mono-glucuronidated gallic

151 acid) suggests glucuronidation at the D-ring (Fig. S2). Similarly, the product ion at *m/z* 359

152 (mono-glucuronidated methyl gallic acid) in MetNeg9 (rt = 5.4 min, *m/z* = 647.128) and
153 MetNeg10 (rt = 4.2 min, *m/z* = 647.128) (tentatively identified as mono-glucuronidated methyl
154 EGCG metabolites) indicates that both methylation and glucuronidation are on the galloyl
155 moiety.

156 Sulfate and glucoside metabolites were also tentatively identified in the negative ion
157 mode (Table 1), which is in agreement with the previous studies [14, 23, 24]. Two tentatively
158 identified mono-sulfated EGCGs (MetNeg1 (rt = 5.4 min, *m/z* = 537.036) and MetNeg2 (rt = 5.1
159 min, *m/z* = 537.038)) with different retention times indicate that the EGCG molecule can have at
160 least two sulfation sites. The product ion pattern of the two tentatively identified mono-sulfate
161 metabolites in the current study were similar to that of EGCG-4″-sulfate reported in a previous
162 study [14]. Those authors identified EGCG-4″-sulfate with a molecular ion *m/z* 537.0347 and
163 product ions at *m/z* 125, 169, and 305, in human plasma after consumption of a green tea
164 catechin-containing beverage. The current results suggest that sulfation occurs at either the 3″- or
165 4″- positions. However, further targeted analysis with a standard compound is required for more
166 accurate identification.

167 Sang et al., identified 2′-cysteinyl EGCG and 2″-cysteinyl EGCG in mouse urine samples
168 after intraperitoneal administration of 200 or 400 mg/kg EGCG [17]. These thiol conjugated
169 metabolites, however, were not found in the present study. This discrepancy may be due to
170 differences in the route of administration used between the current study and this previous work
171 by Sang et al. Intraperitoneal injection is likely to result in the delivery of higher concentrations
172 of EGCG to the liver in a short period of time, because it by-passes the barrier of the small
173 intestine. Indeed, Galati et al., have reported that a single intraperitoneal dose of 100 or 150
174 mg/kg EGCG resulted in increased plasma ALT levels or death, respectively, within 24 h of
175 treatment [25]. Previous studies have shown that single oral bolus dosing with these doses do not
176 cause toxicity [26].

177 In the present study, in the negative ion mode, EGCG quinones were also provisionally
178 identified. Sang et al. first demonstrated the formation of oxidation products *in vitro* but did not
179 detect them in mouse plasma samples after intraperitoneal administration of EGCG (50 mg/kg
180 daily, 3 d) [12]. In the present study, urinary metabolites that were tentatively identified as mono-
181 glucuronidated EGCG quinone, di-glucuronidated EGCG quinone, and EGCG dimer quinone
182 were observed. The first two oxidative products were tentatively identified using both *m/z* values

183 and MS/MS spectra. The EGCG dimer quinone identified in this study appeared to have the
184 same molecular ion as previously reported theasinensin A quinone [12], however, there are
185 discrepancies between the observed and theoretical *m/z* values of these tentatively identified
186 quinones (Table 1). Further target metabolomics studies and preparation of authentic standards
187 are needed to confirm the identities of these metabolites.

188 Both *in vitro* and *in vivo* studies have shown that EGCG can undergo mixed metabolic
189 pathways of methylation, glucuronidation, and sulfation [15, 16, 23]. Our results are consistent with
190 these previous studies. For example, we observed that methylated EGCG conjugated as
191 glucuronides (MetNeg9 (rt = 5.4 min, *m/z* = 647.128), MetNeg10 (rt = 4.2 min, *m/z* = 647.128),
192 MetPos5 (rt = 5.5 min, *m/z* = 649.143), MetPos6 (rt = 4.9 min, *m/z* = 649.143), and MetPos7 (rt
193 = 4.4 min, *m/z* = 649.143)) and sulfates (MetNeg3 (rt = 6.5 min, *m/z* = 551.051)). Di-methylated
194 EGCG was also observed (MetPos2 (rt = 5.3 min, *m/z* = 487.123)). In addition, metabolites with
195 more than two conjugations were also tentatively identified. MetNeg22 (rt = 3.5 min, *m/z* =
196 985.186) showed three neutral losses of glucuronic acid (3 × 176 Da), suggesting it may be a
197 tri-glucuronidated EGCG. To our knowledge, such an EGCG metabolite has not been previously

198 reported, but it seems possible given previous reports of tri- or tetra-glucuronidated quercetin

199 metabolites after supplementation in rats [27].

200

201 *3.2 Comparison of the urinary metabolite profile after EGCG dosing*

202 A total of 4673 and 2891 compounds were detected in negative and positive ion modes,

203 respectively (Fig. 1). A heatmap in negative ion mode clearly shows compounds which increase

204 in a dose-dependent manner, clustered together at the top (Fig. 1A). However, the heatmap also

205 shows that there is biological variation in the urine metabolite profiles of mice, even within the

206 same treatment group. In particular, the urine sample in the first column of the control group in

207 both ion modes showed a different pattern from the other three control samples. The biological

208 differences between urine samples within the same treatment group were greater in the positive

209 ion mode, making the dose-dependent tendency less clear compared to the negative ion mode

210 (Fig. 1B). This variability in EGCG metabolite profiles within the same treatment group may be

211 attributed to stochastic variation in the expression of genes responsible for EGCG metabolism or

212 response to the toxic effects of high doses of EGCG. While an inbred strain of mice (*i.e.*,

213 C57BL/6J) maintained on a semi-purified diet (*i.e.*, AIN93G) was used in the present study,

214 previous studies have shown that transcript levels of genes involved in a wide range of biological
215 functions and in different tissues can vary significantly between mice of the same strain,
216 purchased from the same vendor, and housed under consistent husbandry conditions [28].

217 The results of the PLS-DA in both the negative and positive ion modes show a clear
218 separation in the metabolite profiles of the different treatment groups (Fig. 2A and 2C). The
219 groups were well separated from each other along the first dimension, which explained more
220 than 25% of the total variance in both ion modes. VIP scores were used to identify the
221 compounds driving the separation in the PLS-DA. The peak area of each of the top 20
222 metabolites determined by VIP scores increased dose-dependently in both ion modes (Fig. 2B
223 and 2D). These metabolites can be considered important variables for the discrimination based
224 on the widely accepted 'greater than one rule' criterion for VIP scores [29].

225 Approximately half of the metabolites with the top 20 VIP scores in both ion modes were
226 provisionally identified as EGCG-derived based on their *m/z* values and product ions (Table 2).
227 The metabolite that drives PLS-DA separation in negative ion mode to the greatest extent based
228 on the VIP scores was MetNeg14 (rt = 4.0 min, *m/z* = 806.572), which was tentatively identified
229 as a di-glucuronidated EGCG quinone based on its product ions. This metabolite shares the

230 major fragment ions with the previously reported EGCG quinone [12]. Although not among the top
231 20 metabolites, we also tentatively identified mono-glucuronidated EGCG quinone (VIP rank:
232 290) and EGCG dimer quinone (VIP rank: 155), both of which increased in a dose-dependent
233 manner in mouse urine samples. This indicates EGCG oxidation products are formed at greater
234 levels after the administration of the toxic dose of EGCG. The average peak area of EGCG dimer
235 quinone (MetNeg21 (rt = 4.1 min, *m/z* = 911.112)) and di-glucuronidated EGCG quinone
236 (MetNeg14 (rt = 4.0 min, *m/z* = 806.572)) were more than 100 times higher in the toxic dose
237 group compared to the low dose group (Table 3). Sang et al. proposed that EGCG can be
238 oxidized to form EGCG quinone while generating reactive oxygen species [12]. We have
239 previously reported that the toxic doses of EGCG used in this study can deplete reduced
240 glutathione and induce oxidative stress in the liver [6]. However, as mentioned above, the
241 significant discrepancies between the observed and theoretical *m/z* values of these tentatively
242 identified quinones could indicate that our identification is incorrect. Additional targeted MS/MS
243 analysis are needed to confirm the presence of these biomarkers of oxidative stress.

244 In the positive ion mode, MetPos10 (rt = 1.2 min, *m/z* = 811.159) was the strongest
245 driver for the separation between treatment groups. This compound has a molecular mass which

246 was 352 Da (2 × 176 Da) higher than EGCG. The characteristic ion at *m/z* 635.124 was

247 generated by the neutral loss of one glucuronic acid (176 Da), and a fragment ion at *m/z* 459.091

248 was yielded by the neutral loss of a second glucuronic acid, indicating that this metabolite may

249 be a di-glucuronidated EGCG. Two metabolites tentatively identified as EGCG mono-

250 glucuronide (MetPos3 (rt = 4.6 min, *m/z* = 635.126) and MetPos4 (rt = 4.1 min, *m/z* = 635.126))

251 were also important drivers for the separation between treatment groups in the positive ion mode.

252 In addition, metabolites conjugated with both methylation and glucuronidation pathways were

253 top features driving the PLS-DA separation. MetPos6 (rt = 4.9 min, *m/z* = 649.143) and MetPos7

254 (rt = 4.4 min, *m/z* = 649.143), for example, were tentatively identified as mono-glucuronidated

255 methyl EGCG. The characteristic ions at *m/z* 473 and 649 indicate methyl conjugation (14 Da)

256 and glucuronide conjugation (176 Da), respectively. MetPos12 (rt = 4.9 min, *m/z* = 825.176) and

257 MetPos13 (rt = 4.1 min, *m/z* = 825.177) are also important drivers of separation and were

258 tentatively identified as mono-methylated EGCG diglucuronides.

259 Among the tentatively identified EGCG metabolites in negative ion mode, 10

260 glucuronidation-related metabolites were ranked in the top 100 VIP scores, while only one

261 sulfated metabolite was ranked in the top 100 (Table 1). Together with the observation that all

262 the tentatively identified metabolites among those with the top 20 VIP scores are glucuronidated,
263 these results suggest that glucuronidation may be the key pathway to dealing with toxic doses of
264 EGCG in mice. At high doses of EGCG, glucuronidation may become more predominant than
265 methylation and sulfation due to the higher capacity of glucuronidation as a biotransformative
266 pathway [16, 30]. Hayashi et al. recently reported that the maximum velocity of glucuronidation of
267 EGCG is higher than that of sulfation or methylation in human liver cytosol [14].

268 The potential importance of glucuronidation in dealing with high doses of EGCG may
269 also partially explain the variation in sensitivity between individuals to green tea polyphenols.
270 Previous studies have shown the interindividual differences in the metabolism of green tea
271 polyphenols in both laboratory animals and humans [31, 32]. Lu et al., have reported that human
272 uridine 5′-diphosphate glucuronosyltransferase (UGT)1A8 has a much higher V_{max}/K_m value
273 than other UGT isozymes *in vitro*, indicating that this isoform may play an important role in the
274 biotransformation of EGCG in humans [13]. Genetic polymorphisms have been found in UGT1A8
275 and other isoforms, which can impact the biotransformation and toxicological potential of
276 phenolic compounds [33-35]. In light of this, there may be interindividual variability in the

277 glucuronidation of EGCG which contributes to the sensitivity of certain individuals to EGCG
278 toxicity [36, 37].
279 While PLS-DA results in both ion modes show that EGCG has a dose-dependent effect
280 on the urinary metabolite profile in mice in the first dimension, the treatment groups were not
281 separated in the second dimension. The metabolites aligned in the second dimension may
282 represent the endogenous metabolites that are minimally affected by the EGCG treatment.
283
284 *3.3 Relative quantification of methylated, glucuronidated, and sulfated EGCG metabolites*
285 Since commercially-available, authentic standards were not available for the absolute
286 quantification of EGCG metabolites, we calculated the ratio of the average peak area of each
287 metabolite at the non-toxic and toxic dose for the purpose of relative quantification, focusing on
288 methyl, glucuronide, and sulfate conjugated metabolites (Table 3). The ratio between non-toxic
289 and toxic doses was about twice as large for mono-methylated EGCG (ratio = 24) as for di-
290 methylated EGCG (ratio = 10). This result agrees well with previous studies which found that at
291 low doses, the dimethylated metabolite predominates, whereas at high doses, the
292 monomethylated compound is more abundant [11, 16]. We also observed a similar trend with

293 glucuronidation. The ratio of the peak area of the toxic dose to that of the non-toxic dose was
294 much higher in mono-glucuronidated EGCG (ratio = 13 – 144) compared to di- (ratio = 15 – 45)
295 or tri-glucuronidated EGCG (ratio = 45), especially in negative ion mode. However, one of the
296 mono-glucuronidated EGCG identified in negative ion mode (MetNeg7 (rt = 3.9 min, *m/z* =
297 633.112)) showed a lower ratio compared to the other two, which may indicate a difference in
298 the affinity or capacity for glucuronidation of different sites on EGCG. It has been reported that
299 4″-position is the major glucuronidation site among the observed EGCG glucuronides in *in vitro*
300 studies [13].

301 When comparing methylation and glucuronidation, glucuronidation showed a much
302 higher ratio between toxic and low doses in both mono- and di-conjugated metabolites. The ratio
303 of mono-glucuronidated EGCG was 13 – 144, whereas the ratio of mono-methylated EGCG was
304 24. Similarly, di-glucuronidated EGCG had a ratio of 15 – 45, which was higher than the ratio of
305 10 for di-methylated EGCG. This is consistent with the previous *in vitro* observations that at
306 high EGCG concentrations, glucuronidation may become more dominant than methylation [16].
307 The methylation pathway may become saturated earlier than glucuronidation pathway, resulting
308 in the low ratio of non-toxic to toxic doses. These results indicate the possibility of a shift in the

309 dominant metabolic pathway with increasing dose. The hepatic concentration of *S*-
310 adenosylmethionine (SAM) and uridine diphosphate glucuronic acid (UDPGA) in mice has been
311 reported to be approximately 50 nmol/g and 600 nmol/g, respectively [38, 39]. It is possible that the
312 increasing doses of EGCG lead to the depletion of the hepatic content of SAM, the cofactor for
313 catechol-*O*-methyl transferase (COMT), more rapidly than UDPGA, the cofactor for UGT.
314 Alternatively, EGCG treatment may lead to a more rapid and greater induction of UGT enzyme
315 levels compared to COMT. Further studies to analyze changes in the levels of these enzymes and
316 their cofactors in response to EGCG treatment are needed to better understand the mechanism
317 behind the observed shifts in metabolic pathways.

318 Among three major conjugation types, two mono-sulfated compounds (MetNeg1 (rt = 5.4
319 min, *m/z* = 537.036) and MetNeg2 (rt = 5.1 min, *m/z* = 537.038)) showed the biggest difference
320 between non-toxic and toxic groups (the peak area ratios between non-toxic and toxic doses were
321 391 and 177, respectively). Given that the peak area of the two metabolites was similar in the
322 control and non-toxic groups, we hypothesize that sulfotransferase enzymes may have a lower
323 affinity for EGCG than either COMT or UGT in mice. It has been recently reported that the
324 affinity for EGCG of sulfation was slightly lower than that of methylation but 200-fold higher

325 than that of glucuronidation in human liver cytosol [14]. The discrepancy between this previous
326 study and the present results may indicate species differences in EGCG metabolism and suggest
327 a need for additional studies. Absolute quantification with standards is needed to make more
328 accurate comparisons between the major conjugation pathways at different EGCG dosing levels.
329 The present study has some limitations. First, the lack of commercially-available,
330 authentic standards for EGCG prevented absolute quantification and definitive identification of
331 the metabolites that we detected. Given the large number of metabolites produced, it was also not
332 feasible to synthesize authentic standards for this study. To address this limitation, a relative
333 quantification strategy was employed to examine how changes in dose resulted in changes in
334 metabolite profile. A second limitation was the relatively small number of samples: four
335 biological replicates per treatment. While a larger sample size would allow a better elucidation of
336 variation in metabolite profile, these replicates did each represent the pooled urine of two mice,
337 so the overall differences across treatment groups are representative of a larger number of mice
338 than the number of replicates indicate. In spite of these limitations, the study has several
339 strengths. First, the doses employed have been previously used in pharmacodynamic,
340 metabolism, and toxicology studies, so the results can be considered in the context of those

341 previous studies. Second, samples were analyzed in both the positive and negative ion modes and
342 differences across treatment groups were examined using both known and unknown metabolites
343 and a multivariate statistical analysis approach. Finally, the study generated a large amount of
344 LC-MS/MS data, including both parent compound masses and major fragments, that will support
345 additional future studies on the impact of EGCG on the urine metabolome in mice. Overall, this
346 study shows how the metabolite profile of EGCG differs in mice given a non-toxic oral dose
347 compared to mice given a toxic oral dose. There has been limited information available about the
348 metabolite profile of EGCG at toxic doses. The present study expands previous work on the
349 metabolism of non-toxic doses of EGCG and may contribute to a better understanding of the
350 dose-dependent EGCG-mediated toxicity.
351

352 **4. Conclusions**

353 In summary, we compared the urinary EGCG metabolite profile in mice following
354 treatment with a single oral bolus administration of EGCG at non-toxic or toxic doses, or
355 vehicle. The most important driving metabolites for separation were tentatively identified as di-
356 glucuronidated EGCG quinone and di-glucuronidated EGCG. It is possible that at toxic doses of

357 EGCG, detoxifying biotransformation pathways are overwhelmed, resulting in the formation of
358 EGCG oxidation products that can cause oxidative stress. We also observed that the difference in
359 the formation of metabolites between non-toxic and toxic doses is greatest with sulfation,
360 followed by glucuronidation, and methylation pathway. Although the absolute amounts of the
361 metabolites cannot be compared, the overall results suggest that methylation may have a higher
362 affinity but a lower capacity for EGCG compared to glucuronidation and sulfation. Our results
363 suggest that individuals with chronic elevations in hepatic oxidative stress (e.g., non-alcoholic
364 fatty liver disease, hepatitis, etc.) or with genetic polymorphisms in Phase II metabolism may be
365 susceptible to EGCG toxicity. Further studies with authentic standard compounds and/or targeted
366 MS/MS approaches are needed to achieve a more accurate identification and quantification of
367 EGCG metabolites, and studies in different populations (e.g., obese mice or mice with genetic
368 polymorphisms in Phase II metabolism) are needed to better assess how shifts in the EGCG
369 metabolite profile correlate with sensitivity to EGCG-mediated hepatotoxicity.

Author contributions

CRediT: **Soomee Hwang** formal analysis, visualization, writing-original draft, writing-review & editing; **Imhoi Koo** data curation, visualization, writing-review & editing; **Andrew D. Patterson** resources, writing-review & editing; **Joshua D. Lambert** conceptualization, funding acquisition, writing-review & editing

Conflicts of interest

There are no conflicts to declare.

Acknowledgments

The authors thank Dr. Philip Smith for technical assistance with metabolomics analysis at the Penn State Metabolomics Core Facility. These studies were supported by USDA Hatch grant number PEN04708 (to JDL). SH was supported in part by a University Graduate Fellowship from the Pennsylvania State University.

Abbreviations

ALT, alanine aminotransferase; COMT, catechol-*O*-methyl transferase; EGCG, (-)-epigallocatechin-3-gallate; GTE, green tea extract; MS/MS, tandem mass spectrometry; PLS-DA, partial least squares-discriminant analysis; SAM, *S*-adenosylmethionine; UDPGA, uridine diphosphate glucuronic acid; UGT, uridine 5′-diphosphate glucuronosyltransferase; ULN, upper limit of normal; VIP, variable importance in projection

References

1. Wang, Y. C. & Bachrach, U. The specific anti-cancer activity of green tea (−)-epigallocatechin-3-gallate (EGCG). *Amino Acids.*, 2002, **22**, 131-143, doi:10.1007/s007260200002.

2. Abboud, P. A. *et al.* Therapeutic effect of epigallocatechin-3-gallate in a mouse model of colitis. *European Journal of Pharmacology.*, 2008, **579**, 411-417, doi:https://doi.org/10.1016/j.ejphar.2007.10.053.

3. Isbrucker, R. A., Edwards, J. A., Wolz, E., Davidovich, A. & Bausch, J. Safety studies on epigallocatechin gallate (EGCG) preparations. Part 2: Dermal, acute and short-term toxicity studies. *Food and Chemical Toxicology.*, 2006, **44**, 636-650, doi:https://doi.org/10.1016/j.fct.2005.11.003.

4. Chan, P. C. *et al.* Fourteen-Week Toxicity Study of Green Tea Extract in Rats and Mice. *Toxicologic Pathology.*, 2010, **38**, 1070-1084, doi:10.1177/0192623310382437.

5. Lambert, J. D. *et al.* Hepatotoxicity of high oral dose (-)-epigallocatechin-3-gallate in mice. *Food and Chemical Toxicology.*, 2010, **48**, 409-416, doi:10.1016/j.fct.2009.10.030.

6. James, K. D., Forester, S. C. & Lambert, J. D. Dietary pretreatment with green tea polyphenol, (−)-epigallocatechin-3-gallate reduces the bioavailability and hepatotoxicity of subsequent oral bolus doses of (−)-epigallocatechin-3-gallate. *Food and Chemical Toxicology.*, 2015, **76**, 103-108, doi:https://doi.org/10.1016/j.fct.2014.12.009.

7. James, K. D., Kennett, M. J. & Lambert, J. D. Potential role of the mitochondria as a target for the hepatotoxic effects of (-)-epigallocatechin-3-gallate in mice. *Food and Chemical Toxicology.*, 2018, **111**, 302-309, doi:https://doi.org/10.1016/j.fct.2017.11.029.

8. Hu, J., Webster, D., Cao, J. & Shao, A. The safety of green tea and green tea extract consumption in adults – Results of a systematic review. *Regulatory Toxicology and Pharmacology.*, 2018, **95**, 412-433, doi:https://doi.org/10.1016/j.yrtph.2018.03.019.

9. Dostal, A. M. *et al.* The safety of green tea extract supplementation in postmenopausal women at risk for breast cancer: results of the Minnesota Green Tea Trial. *Food and Chemical Toxicology.*, 2015, **83**, 26-35, doi:10.1016/j.fct.2015.05.019.

10. Li, F. *et al.* Perspectives on the recent developments with green tea polyphenols in drug discovery. *Expert Opinion on Drug Discovery.*, 2018, **13**, 643-660, doi:10.1080/17460441.2018.1465923.

11. Meng, X. *et al.* Identification and Characterization of Methylated and Ring-Fission Metabolites of Tea Catechins Formed in Humans, Mice, and Rats. *Chemical Research in Toxicology.*, 2002,**15**, 1042-1050, doi:10.1021/tx010184a.

12. Sang, S., Yang, I., Buckley, B., Ho, C.-T. & Yang, C. S. Autoxidative quinone formation in vitro and metabolite formation in vivo from tea polyphenol (-)-epigallocatechin-3-gallate: studied by real-time mass spectrometry combined with tandem mass ion mapping. *Free Radical Biology and Medicine.*, 2007, **43**, 362-371, doi:10.1016/j.freeradbiomed.2007.04.008.

13. Lu, H. *et al.* Glucuronides of Tea Catechins: Enzymology of Biosynthesis and Biological Activities. *Drug Metabolism and Disposition.*, 2003, **31**, 452, doi:10.1124/dmd.31.4.452.

14. Hayashi, A. *et al.* 4″-Sulfation Is the Major Metabolic Pathway of Epigallocatechin-3-gallate in Humans: Characterization of Metabolites, Enzymatic Analysis, and Pharmacokinetic Profiling. *Journal of Agricultural and Food Chemistry.*, 2022, **70**, 8264-8273, doi:10.1021/acs.jafc.2c02150.

15. Sang, S., Lambert, J. D., Ho, C.-T. & Yang, C. S. The chemistry and biotransformation of tea constituents. *Pharmacological Research.*, 2011, **64**, 87-99, doi:https://doi.org/10.1016/j.phrs.2011.02.007.

16. Lu, H., Meng, X. & Yang, C. S. Enzymology of methylation of tea catechins and inhibition of catechol-O-methyltransferase by (-)-epigallocatechin gallate. *Drug Metabolism and Disposition.*, 2003, **31**, 572-579, doi:10.1124/dmd.31.5.572.

17. Sang, S. *et al.* Synthesis and Structure Identification of Thiol Conjugates of (−)-Epigallocatechin Gallate and Their Urinary Levels in Mice. *Chemical Research in Toxicology.*, 2005, **18**, 1762-1769, doi:10.1021/tx0501511.

18. Parkinson, A. Biotransformation of xenobiotics, in: Klaassen, C.D. (Ed.), Casarett & Doull's Toxicology: The basic science of poisons, 5th ed., McGraw-Hill, New York, 1996, 113-186.

19. Lambert, J. D., Sang, S., Hong, J. & Yang, C. S. Anticancer and anti-inflammatory effects of cysteine metabolites of the green tea polyphenol, (-)-epigallocatechin-3-gallate. *Journal of Agricultural and Food Chemistry.*, 2010, **58**, 10016-10019, doi:10.1021/jf102311t.

20. Perfetti, X. *et al.* Neurotoxic thioether adducts of 3,4-methylenedioxymethamphetamine identified in human urine after ecstasy ingestion. *Drug Metabolism and Disposition.*, 2009, **37**, 1448-1455, doi:10.1124/dmd.108.026393.

21. Tsugawa, H. *et al.* MS-DIAL: data-independent MS/MS deconvolution for comprehensive metabolome analysis. *Nature Methods.*, 2015, **12**, 523-526, doi:10.1038/nmeth.3393.

22. Pang, Z. *et al.* Using MetaboAnalyst 5.0 for LC–HRMS spectra processing, multi-omics integration and covariate adjustment of global metabolomics data. *Nature Protocols.*, 2022, **17**, 1735-1761, doi:10.1038/s41596-022-00710-w.

23. Kida, K., Suzuki, M., Matsumoto, N., Nanjo, F. & Hara, Y. Identification of Biliary Metabolites of (−)-Epigallocatechin Gallate in Rats. *Journal of Agricultural and Food Chemistry.*, 2000, **48**, 4151-4155, doi:10.1021/jf000386x.

24. Sang, S. & Yang, C. S. Structural identification of novel glucoside and glucuronide metabolites of (-)-epigallocatechin-3-gallate in mouse urine using liquid chromatography/electrospray ionization tandem mass spectrometry. *Rapid Communication in Mass Spectrometry.*, 2008, **22**, 3693-3699, doi:10.1002/rcm.3786.

25. Galati, G., Lin, A., Sultan, A. M. & O'Brien, P. J. Cellular and in vivo hepatotoxicity caused by green tea phenolic acids and catechins. *Free Radical Biology and Medicine* 2006, **40**, 570-580.

26. National Toxicology Program. NTP Technical Report on the Toxicology Studies of Green Tea Extract in F344/NTac Rats and B6C3F1/N Mice and Toxicology and Carcinogenesis Studies of Green Tea Extract in Wistar Han [Crl:WI(Han)] Rats and B6C3F1/N Mice (Gavage Studies): Technical Report 585 [Internet]. Research Triangle Park (NC): National Toxicology Program; 2016 Apr. Available from: https://www.ncbi.nlm.nih.gov/books/NBK561011/ doi: 10.22427/NTP-TR-585.

27. Santos, M. R. *et al.* Influence of the metabolic profile on the in vivo antioxidant activity of quercetin under a low dosage oral regimen in rats. *British Journal of Pharmacology.*, 2008, **153**, 1750-1761, doi:https://doi.org/10.1038/bjp.2008.46.

28. Vedell, P. T., Svenson, K. L. &Churchill, G. A. Stochastic variation of transcript abundance in C57BL/6J mice. *BMC Genomics* 2011, **12**, 167.

29. Vitale, R. *et al.* A rapid and non-invasive method for authenticating the origin of pistachio samples by NIR spectroscopy and chemometrics. *Chemometrics and Intelligent Laboratory Systems.*, 2013, **121**, 90-99, doi:https://doi.org/10.1016/j.chemolab.2012.11.019.

30. Zamek-Gliszczynski, M. J., Hoffmaster, K. A., Nezasa, K.-i., Tallman, M. N. & Brouwer, K. L. R. Integration of hepatic drug transporters and phase II metabolizing enzymes: Mechanisms of hepatic excretion of sulfate, glucuronide, and glutathione metabolites. *European Journal of Pharmaceutical Sciences.*, 2006, **27**, 447-486, doi:https://doi.org/10.1016/j.ejps.2005.12.007.

31. Lee, M.-J. *et al.* Pharmacokinetics of Tea Catechins after Ingestion of Green Tea and (−)-Epigallocatechin-3-gallate by Humans: Formation of Different Metabolites and Individual Variability1. *Cancer Epidemiology, Biomarkers & Prevention.*, 2002, **11**, 1025-1032.

32. Church, R. J. *et al.* Sensitivity to hepatotoxicity due to epigallocatechin gallate is affected by genetic background in diversity outbred mice. *Food and Chemical Toxicology.*, 2015, **76**, 19-26, doi:https://doi.org/10.1016/j.fct.2014.11.008.

33. Ehmer, U. *et al.* Variation of hepatic glucuronidation: Novel functional polymorphisms of the UDP-glucuronosyltransferase UGT1A4. *Hepatology.*, 2004, **39**, 970-977, doi:https://doi.org/10.1002/hep.20131.

34. Jiang, Z. & Hu, N. Effect of UGT polymorphisms on pharmacokinetics and adverse reactions of mycophenolic acid in kidney transplant patients. *Pharmacogenomics.*, 2021, **22**, 1019-1040, doi:10.2217/pgs-2021-0087.

35. Sun, D., Jones, N. R., Manni, A. & Lazarus, P. Characterization of raloxifene glucuronidation: potential role of UGT1A8 genotype on raloxifene metabolism in vivo. *Cancer Prevention Research (Phila).*, 2013, **6**, 719-730, doi:10.1158/1940-6207.Capr-12-0448.

36. Bernard, O., Tojcic, J., Journault, K., Perusse, L. & Guillemette, C. Influence of nonsynonymous polymorphisms of UGT1A8 and UGT2B7 metabolizing enzymes on the formation of phenolic and acyl glucuronides of mycophenolic acid. *Drug Metabolism and Disposition.*, 2006, **34**, 1539-1545, doi:10.1124/dmd.106.010553.

37. Kokawa, Y. *et al.* Effect of UDP-glucuronosyltransferase 1A8 polymorphism on raloxifene glucuronidation. *European Journal of Pharmaceutical Sciences.*, 2013, **49**, 199-205, doi:https://doi.org/10.1016/j.ejps.2013.03.001.

38. Watkins, J. B., Engles, D. R. & Beck, L. V. Effect of volatile anesthetics on the hepatic UDP-glucuronic acid pathway in mice. *Biochemical Pharmacology* 1990, **40**, 731-735.

39. Mantueffel-Cymborowska, M., Chmurzynska, W. & Grzelakowska-Sztabert, B. Tissue-specific effects of testosterone on S-adenosylmethionine formation and utilization in the mouse. *Biochimica et Biophysica Acta (BBA) - General Subjects* 1992, **1116**, 166-172.

Table 1. Mass data of tentatively identified EGCG metabolites

Metabolite ID	*m/z*	RT (min)	Tentative ID	MS/MS* (Relative intensity)	Mass error (ppm)	VIP rank
			Negative ion mode			
	[M-H]⁻					
MetNeg1	537.036	5.4	Mono-sulfated EGCG	536.914 (100); 168.978 (60); 124.997 (18); 456.976 (10); 305.001 (9)	2.9	140
MetNeg2	537.038	5.1	Mono-sulfated EGCG	536.912 (100); 168.978 (86); 124.997 (24); 456.973 (17); 304.999 (15)	6.7	169
MetNeg3	551.051	6.5	Mono-sulfated methyl EGCG	550.926 (100); 470.988 78); 168.977 (28); 186.965 (24); 319.011 (15)	1.6	62
MetNeg4	565.066	8.1	Mono-sulfated di-methyl EGCG	564.936 (100); 484.999 (66); 333.024 (16); 168.977 (14); 124.998 (7)	0.5	201
MetNeg5	631.098	4.4	Mono-glucuronidated EGCG quinone	630.952 (100); 172.954 (32); 211.959 (29); 454.953 (17); 168.973 (15)	6.3	290

MetNeg6	633.112	3.6	Mono-glucuronidated EGCG	632.967 (100); 286.992 (11); 268.986 (10); 462.988 (9); 124.997 (8)	3.6	122
MetNeg7	633.112	3.9	Mono-glucuronidated EGCG	632.969 (100); 168.977 (30); 344.970 (27); 456.975 (19); 304.999 (15)	3.6	135

Table 1. Con't

Metabolite ID	*m/z*	RT (min)	Tentative ID	MS/MS* (Relative intensity)	Mass error (ppm)	VIP rank
			Negative ion mode			
	[M-H]$^-$					
MetNeg8	633.113	4.4	Mono-glucuronidated EGCG	632.968 (100); 168.978 (34); 456.975 (13); 211.957 (12); 344.968 (9)	5.2	29
MetNeg9	647.128	5.4	Mono-glucuronidated methyl EGCG	646.976 (100); 470.984 (73); 168.977 (24); 319.009 (14); 358.978 (9)	4.1	58

MetNeg10	647.128	4.2	Mono-glucuronidated methyl EGCG	646.975 (100); 358.980 (32); 211.957 (9); 470.979 (9); 268.987 (8)	4.1	42
MetNeg11	661.144	5.1	Mono-glucuronidated di-methyl EGCG	660.991 (100); 484.997 (38); 301.002 (9); 182.990 (5); 113.000 (5)	4.5	96
MetNeg12	661.147	6.6	Mono-glucuronidated di-methyl EGCG	n.d.	9.0	173
MetNeg13	795.170	3.9	EGCG mono-glucoside and mono-glucuronide	794.977 (100); 506.979 (19); 344.965 (16); 168.979 (14); 326.960 (10)	9.4	150
MetNeg14	806.572	4.0	Di-glucuronidated EGCG quinone	806.948 (100); 630.953 (58); 344.970 (21); 454.958 (12); 632.966 (11)	-687.0	1

Table 1. Con't

Metabolite ID	*m/z*	RT (min)	Tentative ID	MS/MS* (Relative intensity)	Mass error (ppm)	VIP rank

			Negative ion mode			
	[M-H]$^-$					
MetNeg15	807.169	5.8	Di-glucuronidated EGCG quinone	630.984 (100); 806.977 (97); 454.994 (32); 303.017 (17); 168.978 (10)	53.1	152
MetNeg16	809.147	3.9	Di-glucuronidated EGCG	808.959 (100); 632.964 (49); 344.968 (35); 168.977 (19); 456.972 (10)	6.4	30
MetNeg17	823.162	3.9	Di-glucuronidated methyl EGCG	822.970 (100); 646.976 (28); 470.984 (8); 286.991 (7); 358.982 (6)	5.6	72
MetNeg18	823.162	4.8	Di-glucuronidated methyl EGCG	822.974 (100); 646.977 (74); 470.985 (66); 168.976 (9); 319.013 (7)	5.6	31
MetNeg19	837.178	4.2	Di-glucuronidated di-methyl EGCG	836.983 (100); 660.991 (64); 485.002 (17); 642.985 (5); 301.002 (4)	5.8	36
MetNeg20	837.180	6.0	Di-glucuronidated di-methyl EGCG	836.984 (100); 660.990 (99); 484.997 (75); 418.113 (16); 333.019 (9)	8.2	16
MetNeg21	911.112	4.1	EGCG dimer quinone	n.d.	-21.1	155

Table 1. Con't

Metabolite ID	*m/z*	RT (min)	Tentative ID	MS/MS* (Relative intensity)	Mass error (ppm)	VIP rank
			Negative ion mode			
	[M-H]⁻					
MetNeg22	985.186	3.5	Tri-glucuronidated EGCG	984.947 (100); 808.952 (29); 632.965 (27); 344.968 (24); 520.956 (8)	12.3	157
MetNeg23	999.197	4.4	Tri-glucuronidated methyl EGCG	998.969 (100); 646.981 (54); 822.972 (53); 470.991 (26); 344.970 (22)	7.5	179
			Positive ion mode			
	[M+H]⁺					
MetPos1	473.110	4.4	Mono-methylated EGCG	139.038 (100); 167.033 (18); 289.071 (10); 473.107 (5); 151.037 (4)	4.5	30

MetPos2	487.123	5.3	Di-methylated EGCG	139.039 (100); 153.055 (80); 167.034 (33); 303.086 (21); 487.124 (10)	-1.0	90
MetPos3	635.126	4.6	Mono-glucuronidated EGCG	139.038 (100); 289.071 (27); 151.038 (18); 153.018 (16); 635.126 (11)	2.7	17
MetPos4	635.126	4.1	Mono-glucuronidated EGCG	139.038 (100); 289.071 (25); 153.017 (15); 151.038 (12); 635.126 (12)	2.7	7

Table 1. Con't

Metabolite ID	*m/z*	RT (min)	Tentative ID	MS/MS* (Relative intensity)	Mass error (ppm)	VIP rank
			Positive ion mode			
	[M+H]+					
MetPos5	649.143	5.5	Mono-glucuronidated methyl EGCG	153.054 (100); 303.085 (23); 139.038 (20); 649.140 (16); 138.030 (5)	4.8	22

MetPos6	649.143	4.9	Mono-glucuronidated methyl EGCG	153.054 (100); 139.039 (70); 303.087 (38); 649.142 (25); 473.109 (7)	4.8	18
MetPos7	649.143	4.4	Mono-glucuronidated methyl EGCG	139.038 (100); 289.071 (32); 167.034 (23); 473.109 (14); 649.142 (12)	4.8	10
MetPos8	663.157	4.3	Mono-glucuronidated di-methyl EGCG	153.053 (100); 139.038 (85); 303.086 (82); 487.124 (41); 167.033 (30)	2.1	28
MetPos9	663.159	5.3	Mono-glucuronidated di-methyl EGCG	139.039 (100); 153.055 (85); 303.088 (59); 167.034 (34); 487.124 (25)	5.2	13
MetPos10	811.159	1.2	Di-glucuronidated EGCG	139.038 (100); 289.070 (64); 635.124 (52); 811.154 (46); 153.018 (17)	3.2	1

Table 1. Con't

Metabolite ID	*m/z*	RT (min)	Tentative ID	MS/MS* (Relative intensity)	Mass error (ppm)	VIP rank
			Positive ion mode			
	[M+H]+					
MetPos11	811.159	4.1	Di-glucuronidated EGCG	139.038 (100); 811.159 (80); 289.071 (69); 635.130 (68); 811.363 (23)	3.2	34
MetPos12	825.176	4.9	Di-glucuronidated methyl EGCG	303.086 (100); 153.054 (95); 649.139 (76); 139.038 (57); 825.173 (50)	4.9	8
MetPos13	825.177	4.1	Di-glucuronidated methyl EGCG	139.038 (100); 289.071 (66); 649.139 (50); 473.107 (45); 825.173 (30)	6.1	12

* The first five fragment ions with the highest relative intensity were shown for MS/MS data; n.d.: not detected

Table 2. The top 20 metabolites ranked by the variable importance in projection (VIP) scores

Metabolite ID	*m/z*	RT (min)	Tentative ID*	MS/MS** (Rel. intensity)
			Negative ion mode	
	[M-H]⁻			
MetNeg14	806.572	4.0	Di-glucuronidated EGCG quinone	806.948 (100); 630.953 (58); 344.970 (21); 454.958 (12); 632.966 (11)
MetNeg24	1050.184	4.2	Unknown EGCG metabolite	1049.942 (100); 836.985 (99); 211.955 (37); 660.989 (37); 484.998 (9)
MetNeg25	1214.229	4.0	Unknown	n.d.
MetNeg26	1041.151	3.9	Unknown EGCG metabolite	1040.908 (100); 808.959 (64); 230.945 (48); 632.964 (26); 344.968 (10)
MetNeg27	1044.132	3.2	Unknown	820.956 (100); 945.938 (81); 1043.887 (53); 644.962 (21); 344.971 (19)
MetNeg28	1217.195	3.4	Unknown	n.d.
MetNeg29	935.146	6.0	Unknown	836.980 (100); 660.991 (81); 934.924 (69); 484.993 (42); 333.023 (6)
MetNeg30	1178.169	3.2	Unknown	820.954 (100); 1177.900 (77); 945.947 (51); 644.964 (24); 344.966 (12)

MetNeg31	910.118	3.9	Unknown	n.d.
MetNeg32	731.082	4.4	Unknown EGCG metabolite	632.963 (100); 168.977 (48); 730.908 (36); 456.972 (28); 344.968 (22)

Table 2. Con't

Metabolite ID	*m/z*	RT (min)	Tentative ID*	MS/MS** (Rel. intensity)
			Negative ion mode	
	[M-H]-			
MetNeg33	983.148	4.0	Unknown EGCG metabolite	808.960 (100); 982.918 (85); 632.966 (46); 344.968 (22); 172.953 (17)
MetNeg34	947.178	5.8	Unknown EGCG metabolite	946.953 (100); 770.970 (19); 344.965 (17); 821.945 (5); 632.964 (4)
MetNeg35	1071.165	4.0	Unknown	n.d.
MetNeg36	929.094	4.0	Unknown EGCG metabolite	830.933 (100); 928.879 (81); 366.943 (46); 542.935 (18); 654.938 (14)

MetNeg37	921.128	3.4	Unknown EGCG metabolite	822.969 (100); 920.926 (82); 646.982 (28); 358.981 (27); 534.972 (11)
MetNeg20	837.180	6.0	Di-glucuronidated di-methyl EGCG	836.984 (100); 660.990 (99); 484.997 (75); 418.113 (16); 333.019 (9)
MetNeg38	1086.219	4.1	Unknown EGCG metabolite	808.957 (100); 1085.966 (99); 632.966 (37); 344.968 (16); 275.993 (11)
MetNeg39	745.094	4.2	Unknown	646.975 (100); 744.920 (57); 358.980 (45); 96.939 (25); 470.984 (14)
MetNeg40	874.152	5.1	Unknown	211.955 (100); 873.953 (61); 873.911 (8); 369.980 (8); 660.971 (5)
MetNeg41	1057.176	3.9	Unknown	n.d.

Table 2. Con't

Metabolite ID	*m/z*	RT (min)	Tentative ID*	MS/MS** (Rel. intensity)
			Positive ion mode	
	$[M+H]^+$			

MetPos10	811.159	1.2	Di-glucuronidated EGCG	139.038 (100); 289.070 (64); 635.124 (52); 811.154 (46); 153.018 (17)
MetPos14	1073.292	4.4	Unknown	263.140 (100); 1073.290 (74); 116.070 (6); 120.080 (4); 262.313 (1)
MetPos15	828.186	4.1	Unknown EGCG metabolite	139.038 (100); 289.071 (76); 635.125 (75); 828.181 (43); 811.155 (40)
MetPos16	833.140	4.1	Unknown	833.137 (100); 481.074 (82); 657.107 (54); 311.050 (3); 343.044 (1)
MetPos17	1086.283	4.6	Unknown	276.127 (100); 1086.283 (66); 259.100 (40); 181.086 (12); 163.075 (6)
MetPos18	871.191	4.1	Unknown EGCG metabolite	139.038 (100); 635.128 (77); 289.073 (70); 811.162 (58); 153.018 (12)
MetPos4	635.126	4.1	Mono-glucuronidated EGCG	139.038 (100); 289.071 (25); 153.017 (15); 151.038 (12); 635.126 (12)
MetPos12	825.176	4.9	Di-glucuronidated methyl EGCG	303.086 (100); 153.054 (95); 649.139 (76); 139.038 (57); 825.173 (50)
MetPos19	842.202	5.0	Unknown EGCG metabolite	303.087 (100); 649.142 (94); 153.054 (84); 139.038 (61); 842.200 (41)

Table 2. Con't

Metabolite ID	*m/z*	RT (min)	Tentative ID*	MS/MS** (Rel. intensity)
			Positive ion mode	
	[M+H]+			
MetPos7	649.143	4.4	Mono-glucuronidated methyl EGCG	139.038 (100); 289.071 (32); 167.034 (23); 473.109 (14); 649.142 (12)
MetPos20	849.117	4.1	Unknown	849.118 (100); 673.083 (50); 497.053 (13); 453.080 (3); 629.113 (1)
MetPos13	825.177	4.1	Di-glucuronidated methyl EGCG	139.038 (100); 289.071 (66); 649.139 (50); 473.107 (45); 825.173 (30)
MetPos9	663.159	5.3	Mono-glucuronidated di-methyl EGCG	139.039 (100); 153.055 (85); 303.088 (59); 167.034 (34); 487.124 (25)
MetPos21	865.078	4.1	Unknown	n.d.
MetPos22	1084.261	4.3	Unknown	n.d.
MetPos23	911.274	4.4	Unknown	263.140 (100); 911.444 (24); 911.275 (21); 116.070 (9); 120.080 (6)
MetPos3	635.126	4.6	Mono-glucuronidated EGCG	139.038 (100); 289.071 (27); 151.038 (18); 153.018 (16); 635.126 (11)

MetPos6	649.143	4.9	Mono-glucuronidated methyl EGCG	153.054 (100); 139.039 (70); 303.087 (38); 649.142 (25); 473.109 (7)
MetPos24	657.109	4.6	Unknown	657.107 (100); 481.074 (62); 263.142 (2); 657.208 (2); 311.049 (1)
MetPos25	842.202	4.1	Unknown	n.d.

[*] Metabolites that are sharing the characteristic product ion with EGCG were considered unknown EGCG metabolites

[**] The first five fragment ions with the highest relative intensity were shown for MS/MS data; n.d.: not detected

Table 3. The ratio of the peak area between non-toxic and toxic doses

Metabolite ID	*m/z*	RT (min)	Tentative ID	Ratio*
EGCG	459.093	4.4	Epigallocatechin-3-gallate (Pos.)	3
EGCG	457.079	4.2	Epigallocatechin-3-gallate (Neg.)	3
			Oxidation Products	
MetNeg5	631.098	4.4	Mono-glucuronidated EGCG quinone	15
MetNeg14	806.572	4.0	Di-glucuronidated EGCG quinone	368
MetNeg15	807.169	5.8	Di-glucuronidated EGCG quinone	27
MetNeg21	911.112	4.1	EGCG dimer quinone	155
			Methylated Products	
MetPos1	473.110	4.4	Mono-methylated EGCG	24
MetPos2	487.123	5.3	Di-methylated EGCG	10
			Glucuronidated Products	
MetPos3	635.126	4.6	Mono-glucuronidated EGCG	46
MetPos4	635.126	4.1	Mono-glucuronidated EGCG	32
MetNeg6	633.112	3.6	Mono-glucuronidated EGCG	123
MetNeg7	633.112	3.9	Mono-glucuronidated EGCG	13
MetNeg8	633.113	4.4	Mono-glucuronidated EGCG	144
MetPos11	811.159	4.1	Di-glucuronidated EGCG	45
MetPos10	811.159	1.2	Di-glucuronidated EGCG	15

MetNeg16	809.147	3.9	Di-glucuronidated EGCG	37
MetNeg22	985.186	3.5	Tri-glucuronidated EGCG	45
			Sulfated Products	
MetNeg1	537.036	5.4	Mono-sulfated EGCG	391
MetNeg2	537.038	5.1	Mono-sulfated EGCG	177

* The averaged peak area for each treatment group was used for calculating the ratio between non-toxic and toxic doses.

Figure Legends

Figure 1. Clustering analysis of mouse urine metabolites after oral dosing EGCG. Male C57BL/6J mice were given a single intragastric dose of EGCG at 100 mg/kg body weight (non-toxic) or 750 mg/kg body weight (toxic), or 0.9% NaCl (vehicle). Metabolomic data from urine after dosing were collected in both the (A) negative and (B) positive ion modes. Cluster analysis was performed using MetaboAnalyst 5.0 and distance measuring was based on Euclidean distance using Ward clustering. Analysis was performed on 4 pooled urine samples for each treatment group. Pooled urine samples represent 2 mice.

Figure 2. Multivariate analysis of mouse urine metabolites after oral dosing EGCG. Male C57BL/6J mice were given a single intragastric dose of EGCG at 100 mg/kg body weight (non-toxic) or 750 mg/kg body weight (toxic), or 0.9% NaCl (vehicle). Partial least squares-discriminant analysis (PLS-DA). Scores plots were prepared using MetaboAnalyst 5.0 for metabolomics data collected in both the (A) negative and (C) positive ion modes. The first 20 important metabolites ranked by the variable importance in projection (VIP) scores were determined for data from the (B) negative and (D) positive ion mode. Analysis was performed on 4 pooled urine samples for each treatment group. Pooled urine samples represent 2 mice. The description of the metabolites can be found in Table 2.

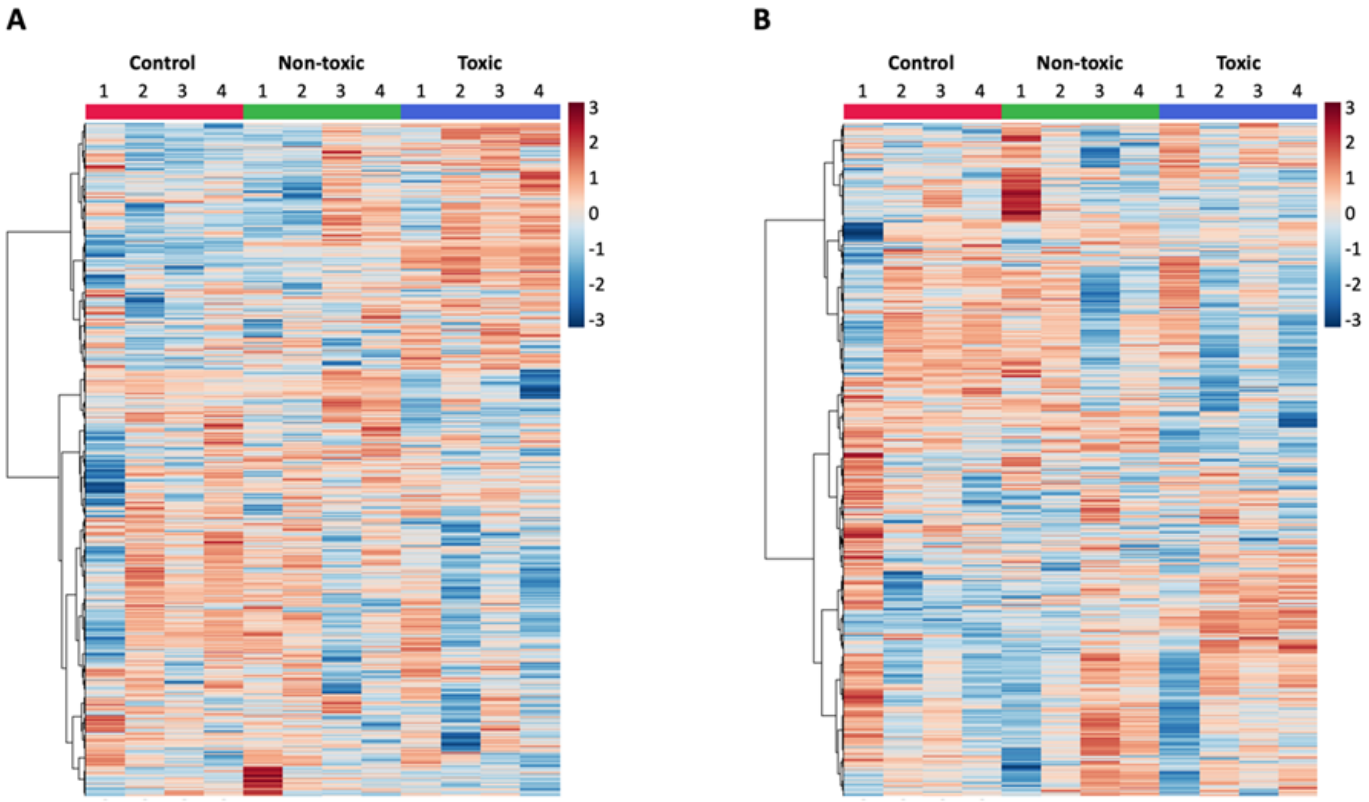
A
Control
Non-toxic
Toxic
1 2 3 4 1 2 3 4 1 2 3 4
3
2
1
0
-1
-2
-3
B
Control
Non-toxic
Toxic
1 2 3 4 1 2 3 4 1 2 3 4
3
2
1
0
-1
-2
-3

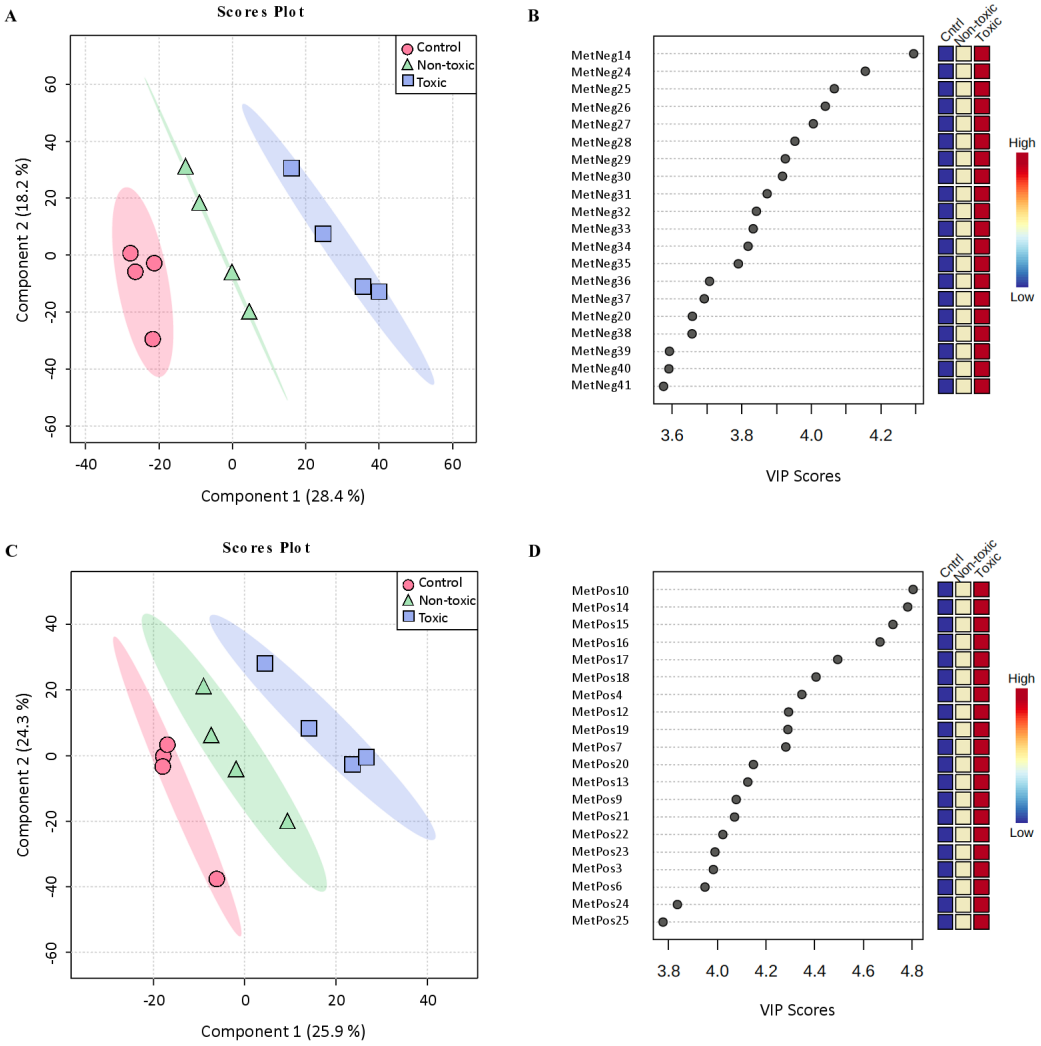
A
Scores Plot
Control
Non-toxic
Toxic
Component 2 (18.2 %)
Component 1 (28.4 %)
B
Cntrl
Non-toxic
Toxic
MetNeg14
MetNeg24
MetNeg25
MetNeg26
MetNeg27
MetNeg28
MetNeg29
MetNeg30
MetNeg31
MetNeg32
MetNeg33
MetNeg34
MetNeg35
MetNeg36
MetNeg37
MetNeg20
MetNeg38
MetNeg39
MetNeg40
MetNeg41
High
Low
VIP Scores
C
Scores Plot
Control
Non-toxic
Toxic
Component 2 (24.3 %)
Component 1 (25.9 %)
D
Cntrl
Non-toxic
Toxic
MetPos10
MetPos14
MetPos15
MetPos16
MetPos17
MetPos18
MetPos4
MetPos12
MetPos19
MetPos7
MetPos20
MetPos13
MetPos9
MetPos21
MetPos22
MetPos23
MetPos3
MetPos6
MetPos24
MetPos25
High
Low
VIP Scores